Pressure-induced structural changes in ZnS

Serge Desgreniers, Luc Beaulieu,* and Ian Lepage
Institut de Physique Ottawa-Carleton, Université d'Ottawa, Département de physique, Ottawa, Ontario, Canada K1N 6N5
(Received 6 October 1999)

We report detailed data on the structural parameters and equations of state of high-density ZnS obtained by x-ray diffraction using synchrotron radiation for pressures below 96 GPa. It is shown that initial room condition phases of ZnS, zinc blende and wurtzite, transform unambiguously to the rocksalt structure at 12 GPa and at room temperature. Our data hence rule out the existence of an intermediate phase of the cinnabar type in ZnS. The initial zinc-blende and wurtzite phases present quantitatively similar equations of state parametrized by $B_0=79.5$ GPa and $B_0'=4$, and $B_0=80.1$ GPa and $B_0'=4$, respectively. As compared to the initial phases, the rocksalt phase, adopted at higher pressure, is denser and less compressible with $B_0=117.6$ GPa and $B_0'=4$. The high-pressure rocksalt structure is also shown to be unstable for pressures in excess of 65 GPa, leading to a transition to the $Cmcm$ structure, an orthorhombic distortion, without a significant change in volume. The occurrence of the $Cmcm$ structure in dense ZnS is in line with the observed dense phases in other zinc chalcogenides.

I. INTRODUCTION

Zinc sulfide adopts two archetypal crystalline structures at room conditions, namely, wurtzite ($P6_3mc$, $Z=2$) and zinc blende ($F\bar{4}3m$, $Z=2$). The tetrahedron formed by the Zn atoms and its four first neighbor S atoms in the wurtzite structure is almost identical to what is observed in the zinc-blende structure. Furthermore, a large fraction [9 out of 12 (Ref. 1)] of the second-alike neighbors are the same in both structures. Consequently, the unit-cell volume difference between the two structures is slim and one expects their compressive properties to be comparable. Zinc sulfide has been studied repeatedly at high pressure. Chang and Barsh[1] measured, by ultrasound propagation, the equation of state of zinc blende ZnS. A first phase transition from zinc blende to rocksalt ($Fm3m$) was reported in several studies.[2–4] More recently, the structural, optical, and electronic properties of cubic (zinc blende) ZnS were studied by Ves *et al.*[5] and Zhou, Campbell, and Heinz.[6] In both studies, equations of state for both the zinc-blende and the higher density rocksalt phases were reported, with a reduced number of data points for the high-density phase resulting in a less than accurate equation of state. The rocksalt phase has been reported to be stable to 45 GPa;[6] a further transition to a distorted rocksalt structure has been observed above 64 GPa,[7] a result not supported by the static pressure results of the recent study of Uchino *et al.*[8] In the latter study, indications of melting or decomposition over 75 GPa and a temperature in excess of 3300 K, resulting from dynamic compression, were also reported. Several computational studies have also produced numerical estimates for the pressure range of phase stability, transition volumes and pressures, and compression parameters of dense ZnS. By first-principles Hartree-Fock calculations, Jaffe, Pandey, and Seel[9] have obtained structural and compression parameters which agree favorably with the so far published experimental results. Recio, Pandey, and Luaña[10] have also calculated the structural and equation of state parameters of the rocksalt phase, by the *ab initio* perturbed-ion method, and found a quantitative agreement with the $P(V)$ experimental results of Zhou, Campbell, and Heinz,[6] at least using an equation of state formalism derived from finite strain theory. Moreover, a first calculation of Nazzal and Qteish[11] have implied the occurrence of a cinnabar-type phase as an intermediate step between the lower density zinc-blende structure and the higher density rocksalt structure. Recent and more accurate calculations[12] have indicated that the cinnabar structure is unstable in the pressure range close to the pressure of the wurtzite-rocksalt transition. In view of the available structural and compression data of dense ZnS and the current understanding of the material, we have defined four goals for the present x-ray-diffraction study: (1) establish the stability of the high-pressure, high-density phases of ZnS at room temperature; (2) measure accurately the structural parameters and the equations of state of ZnS in the zinc-blende, wurtzite, and rocksalt phases and compare then with the calculated ones; (3) search for the existence of a presumed cinnabar-type phase, intermediate to the low-pressure zinc-blende and the high-pressure rocksalt structures; and (4) confirm and characterize the distortion of the high-density rocksalt phase occurring at very high pressure. The pressure-induced transitions in ZnS recorded in the present study are summarized in Fig. 1.

II. EXPERIMENT

Polycrystalline samples from two sources were used in this study: synthetic ZnS with a nominal purity of 99.999% (Alfa AESAR) and a fine powder prepared from a natural ZnS crystal (unknown provenance). Synthetic ZnS was in the wurtzite phase. It should be mentioned that in an attempt to reduce the synthetic sample to a finer powder by grinding, the sample partially transformed to the zinc-blende structure resulting in a rich wurtzite/poor zinc-blende mixture. Powdered natural ZnS was confirmed to be in the zinc-blende structure only. Room condition structural parameters of all samples used in this study and measured *in situ* are given in

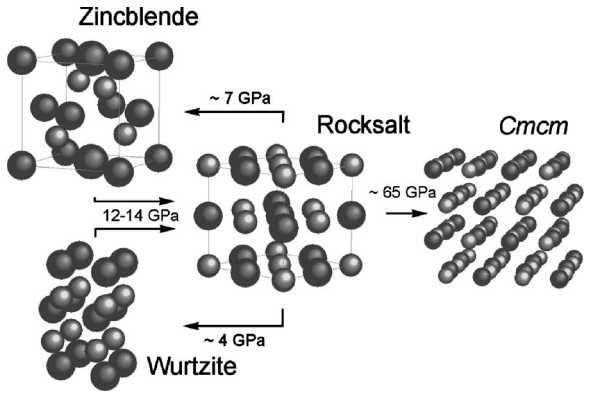

FIG. 1. Pressure-induced structural transformations in ZnS found in the present study. A room condition mixture of wurtzite and zinc blende ZnS (powder sample) transforms to the rocksalt structure between 12 and 14 GPa, respectively. Upon pressure release, ZnS reverts to the wurtzite and zinc-blende phases at different pressures. Above ~65 GPa, rocksalt ZnS further transforms to an orthorhombically distorted structure (*Cmcm*) depicted here.

Table I; they were found in good agreement with those published in the literature. Samples were loaded in gasketed diamond-anvil cells using silicone fluid (Dow Corning 704) as a pressure transmitting medium for generating pressures in excess of 95 GPa. Fine Cu powder, mixed along with the sample, was used as a pressure gauge. Our pressure calibration was based on the available shock compression data of pristine Cu,[13–15] fitted to a Birch-Murnaghan equation of state ($V_0 = 47.23$ Å^3/unit cell, $B_0 = 129.497$ GPa, and $B_0' = 3.346$) for the purpose of volume-pressure interpolation.

Energy dispersive x-ray diffraction experiments (EDXD) were carried out at the National High Pressure Facility of CHESS (Cornell High Energy Synchrotron Source, B1 line).[16] The angle calibration was obtained from x-ray diffraction of a thin Au foil, accurately located at the sample position. All EDXD spectra were acquired at either $E \cdot d = 40.28 \pm 0.05$ keV Å or $E \cdot d = 64.861 \pm 0.005$ keV Å. Angle dispersive x-ray-diffraction experiments (ADXD) were carried out at the CHESS F2 station using monochromatic radiation at 0.3099 Å (obtained from a wiggler and a double-bounced Si(111) monochromator, sagittally focused at the sample) and the CHESS B2 station with 0.4959 Å radiation [obtained from the bending magnet and a double-bounced Si(111) monochromator]. X-ray-diffraction images were recorded on Fuji HRIII imaging plates, placed typically at 29 cm from the sample location. After x-ray exposures ranging from 15 to 30 min at F2 and 90 to 120 min at B2, imaging plates were read by a Fuji BAS2000 scanner at 100-μm^2 pixel resolution. X-ray-diffraction images were processed using the program SImPA (Ref. 17) to obtain 2-θ patterns from a proper azimuthal integration of the Debye diffraction rings. For both EDXD and ADXD experiments, appropriate x-ray beam collimation was provided by crossed microslabs of tungsten defining a nearly square 900-μm^2 beam. All x-ray-diffraction spectra were exempt of signal from the gasket material used to constrain the sample at high pressure. X-ray-diffraction spectra were analyzed using the program XRDA.[18,19] DBWS9411 (Ref. 20) was also used for structure refinements.

III. RESULTS AND DISCUSSION

A. Crystalline structure sequence under pressure, below 65 GPa

Structural transformations were induced by starting from different samples and preparations. In all samples, whether the initial phase is wurtzite, zinc blende, or a mixture of the these two phases, the ultimate structure is rocksalt for pressures below 65 GPa. When starting from the pure wurtzite phase (sample 4), the sample transforms to the zinc-blende structure prior to a transition at higher pressure to the rocksalt structure with coexistence of both the zinc blende and the rocksalt over pressures ranging from 12.4 to 13.5 GPa. With an initial pure zinc-blende phase (samples 3 and 5), ZnS proceeds under pressure to coexisting phases of zinc blende and rocksalt, from approximately 8 to 13 GPa, and to the rocksalt structure only at a pressure larger than 13 GPa. With samples initially showing both wurtzite and zinc-blende structure (samples 1 and 2), the transformation to the zinc-blende structure (with a weak component of the wurtzite phase in sample 1) is observed prior to a complete transition to rocksalt structure. In the case of samples 1 and 2, pressures at which the onset of the rocksalt structure is observed range from 12.5 to 20 GPa, with a dominant pressure centered around 13 GPa. Although the transition from zinc blende to rocksalt is of first order, the relatively extended pressure range over which the transition is observed is indicative of uncertainties in local pressure estimation due to the coexistence two phases having a large volume difference, stress field conditions, and sample preparation. Pressure-induced structural transformations were recorded by starting from different samples and preparations. Typical ADXD patterns are illustrated in Fig. 2. Table II summarizes the transition pressures and the pressure range of stability of all phases observed at room temperature. Our observations of

TABLE I. Room condition structural parameters of ZnS samples used in this study. Labels are used for reference in text and figures. As indicated, both energy dispersive (EDXD) and angle dispersive (ADXD) x-ray-diffraction methods were used. The wurtzite *u* positional parameter is calculated according to the ideal relationship $uc/a = (\frac{3}{8})^{1/2}$.

Sample	Structure	Diffraction method	*a* (Å)	*c* (Å)	*u*
1 - synthetic	wurtzite, zinc blende	EDXD	3.816, 5.395	6.252	0.374
2 - synthetic	wurtzite, zinc blende	EDXD	3.816, 5.395	6.252	0.374
3,5 - natural	zinc blende	EDXD, ADXD	5.410		
4 - synthetic	wurtzite	EDXD, ADXD	3.816	6.252	0.374

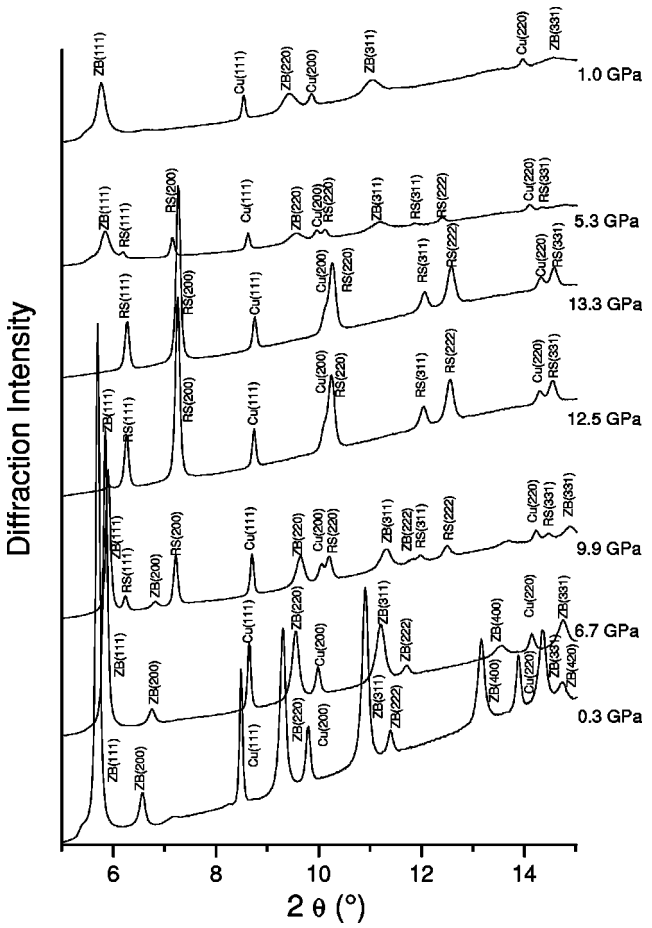

FIG. 2. Room-temperature ADXD patterns of ZnS (sample 3) at selected pressures indicating the evident pressure-induced transition from the zinc-blende (ZB) to the rocksalt (RS) structure and the back transformation to zinc blende. Patterns have been shifted vertically for clarity. Pressure increases and then decreases from bottom to top. X-ray-diffraction lines of Cu are used here for pressure calibration. The stability of other phases in the same pressure range, e.g., an intermediate cinnabar phase, is ruled out.

pressure-induced transitions and the measurements of transition pressures and volumes changes are in agreement with those stated in other reports.[21,1,5,6]

B. Equations of state for phases occurring below 65 GPa

From the volume-pressure experimental data for the wurtzite, zinc-blende, and rocksalt structures, we have obtained the respective equations of state. Our results are summarized in Table III. We have chosen to use the Birch-Murnaghan formalism to extract the room pressure compression parameters, i.e., the atomic volume (V_0), the bulk modulus (B_0), and its pressure derivative, $[(\partial(B_0)/\partial P]_T = B_0'$. Proven to give good estimates of the compression parameters in numerous instances, the Birch-Murnaghan equation of state is expressed by

$$P = \frac{3B_0}{2}\left[\left(\frac{V}{V_0}\right)^{7/3} - \left(\frac{V}{V_0}\right)^{5/3}\right]\left\{1 + \frac{3}{4}(B_0' - 4)\left[\left(\frac{V}{V_0}\right)^{2/3} - 1\right]\right\}.$$

The compression parameters are obtained by a standard weighted χ^2 minimization to the Birch-Murnaghan equation of state. The initial volume V_0 is taken as an adjustable parameter for the occurrence of a phase not stable at ambient conditions, as for the case of the high-pressure rocksalt phase.

The low-density phases of ZnS, namely, wurtzite and zinc blende, are very similar in terms of their compression properties as illustrated in Fig. 3. Room condition unit-cell volumes are close for both phases (for synthetic samples, 39.2 and 38.9 Å^3, respectively), both phases transform to the higher density rocksalt phase, and the change of relative volumes as a function of pressure is nearly identical. Our results are in line with the fact that the Zn coordination is almost identical in both wurtzite and zinc-blende structures. Figure 4 shows experimental volume data obtained from three different loadings of synthetic ZnS and plotted as a function of increasing pressure. Error bars were omitted in Fig. 4 as to present clearly the numerous data points. Estimated errors on volumes are typically of the order to the symbol size whereas those on pressures are within 3%, mainly due to nonhydrostatic conditions. The large number of data points allows a good estimation of the compression parameters. By constraining the pressure derivative of the room pressure bulk modulus $[\partial(B_0)/\partial P]_T$, at a value of 4, we have obtained bulk moduli B_0 of 80.1 and 79.5 GPa, for the wurtzite and the zinc-blende phases of synthetic samples, respectively. For natural ZnS in the zinc-blende structure, the B_0 with a $[\partial(B_0)/\partial P]_T$ of 4, calculated with a far fewer number of points, is close to 86 GPa.

From the zinc-blende phase, ZnS proceeds to the cubic rocksalt phase with in a pressure range over which both phases coexist. From 20 GPa (in all samples) up to

TABLE II. Phases observed and their associated transition pressures or pressure ranges for all samples studied. W, ZB, RS, and DRS stand for wurtzite, zinc blende, rocksalt, and distorted rocksalt, respectively. Phase mixture components are listed by order of importance and are separated by a +. P_{max} indicates the maximum pressure at which a given sample was submitted. All pressures are in units of GPa.

		W	W+ZB	ZB	W+ZB+RS	ZB+RS	RS	DRS	RS	RS+ZB	RS+ZB+W	ZB+W	ZB
Sample	P_{max}				Increasing pressure						Decreasing pressure		
1	61		room		14.1–14.6		16.8–20.0				10.9–10.0	7.6–6.7	
2	20.8		room	8.7–9.4		12.3–12.9	16.3–17.3			11.6–10.3			4.9–4.3
3	14.4			room		7.7–8.3	12.5–13.3		8.3–6.7				4.1–2.4
4	16.3	room		10.7–11.4		12.4	13.5			*n/d*			10.4–4.7
5	96			room		12.3	13.5	~65	74.8	*n/d*			3.9

TABLE III. Compression parameters for dense ZnS in the wurtzite, zinc-blende, and rocksalt structures, as obtained from x-ray diffraction experiments and computer simulations. V_0, B_0, and $(V/V_0)_{Tr}$ stand for the initial atomic volume, the bulk modulus extrapolated to room pressure, and relative unit-cell volume at a transition pressure, respectively. Subscript 0, Tr↑, and Tr↓ refer to room conditions and uploading transition, and downloading transition, respectively. cst indicates that the parameter was held constant in the fit.

Sample phase	Results	V_0 (Å^3)	B_0 (GPa)	$[\partial(B_0)/\partial P]_T$	$(V/V_0)_{Tr}$	$P_{Tr\uparrow}$ (GPa)	$P_{Tr\downarrow}$ (GPa)
Natural zinc blende	present	39.75	86, 92	4 (cst), 2.3			
Natural rocksalt	present	32.3	137.2, 147	4(cst), 2.4	0.814	8.2	6.5
Synthetic zinc blende	present	38.9	79.5	4(cst)			
	expt.	39.65[a]; 39.61[g]	75.0[a]; 76.5[g]	4(cst)[a]; 4.49[g]			
	simul.	39.23[a]; 43.44[c]	82.0[a]; 75.9[c]	4.20[a]; 4.7[c]	0.853[a]; 0.862[c]		
		39.56[d]; 36.81[e]	83.2[d]; 83.3[e]	4.43[d]; 3.92[e]			
Synthetic wurtzite	present	39.2	80.1	4 (cst)			
	expt.	39.61[g]	75.8[g]	4.41[g]			
Synthetic rocksalt	present	31.6	117.6, 96.2	4(cst), 4.35	0.821, 0.830	14.6	10.0
	expt.	32.38[a]; 33.61[f]	103.6[a]; 85.0[f]	4(cst)[a]; 4 (cst)[f]	0.865[a]; 0.851[f]	14.7[a]; ~11[f]	
	simul.	33.05[a]; 33.65[b]; 35.36[c]	100.1[a]; 81[b]; 83.1[c]	4.05[a]; 4.1[b]; 10.0[c]	0.84[a]; ~0.85[b]; 0.89[c]	19.5[a]; 11.2[b]; 16.1[c]	
		31.6[d]; 30.3[e]	104.4[d]; 107.6[e]	4.29[d]; 4.1[e]		14.7[d]; 14.5[e]	

[a]LMTO-LDA total-energy calculations; x-ray-diffraction results, Murnaghan equation of state (Ref. 5).
[b]*Ab initio* perturbed-ion calculations (Ref. 10).
[c]*Ab initio* Hartree-Fock calculations (Ref. 9).
[d]*Ab initio* pseudopotentials, relaxed *d* electrons (Ref. 11).
[e]*Ab initio* pseudopotentials, frozen *d* electrons (Ref. 11).
[f]Derived from x-ray-diffraction data, first-order Birch-Murnaghan equation of state (Ref. 6).
[g]Derived from ultrasonic data (Ref. 1).

~65 GPa, ZnS is stable in the rocksalt structure. The relative change of volume with increasing pressure is plotted in Fig. 4 for both the initial phase and the denser rocksalt phase. A large relative volume change is measured as the transition is recorded, of the order of 17%, in agreement with figures reported in the literature.[5,6] The volume data corresponding to the rocksalt fitted to the Birch-Murnaghan equation of state leads to $B_0 = 117.6$ GPa and an extrapolated room pres-

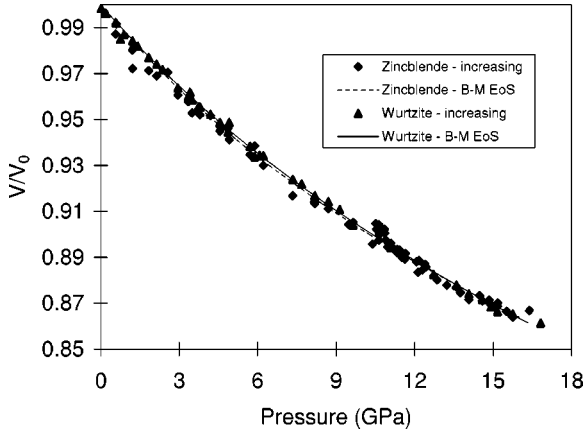

FIG. 3. Experimental equations of state of wurtzite and zinc blende ZnS. Data were recorded for increasing pressures from a synthetic, wurtzite-rich and zinc-blende-poor ZnS sample. All data for wurtzite (solid triangles) and the zinc-blende (solid diamonds) phases are fitted to Birch-Murnaghan equations of state, plotted here as solid lines. Fitting parameters are those given in Table III.

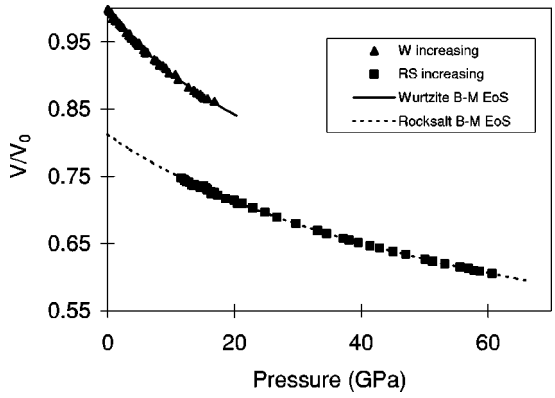

FIG. 4. Experimental equations of state of synthetic ZnS powder. Data points were collected upon pressure increase from three different runs of the same synthetic powder using ADXD and EDXD techniques. All data of the low-pressure wurtzite phase (solid triangles) and the high-pressure rocksalt phase (solid squares) are fitted to Birch-Murnaghan equations of state, plotted here as solid lines. Fitting parameters are those given in Table III.

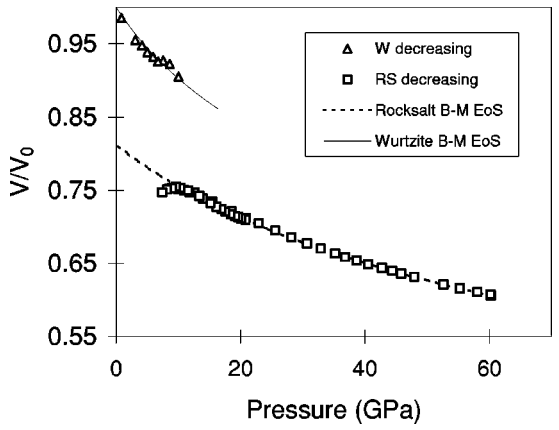

FIG. 5. Volume-pressure data points recorded from one synthetic sample (sample 1) upon pressure decrease for the high-pressure rocksalt phase (open squares) and low-pressure wurtzite phase (open triangles). Lines correspond to Birch-Murnaghan equations of state obtained from volume-pressure data points recorded upon increasing pressure, exactly as shown in Fig. 4. Significant deviations are thus observed over the pressure range where the two phases coexist.

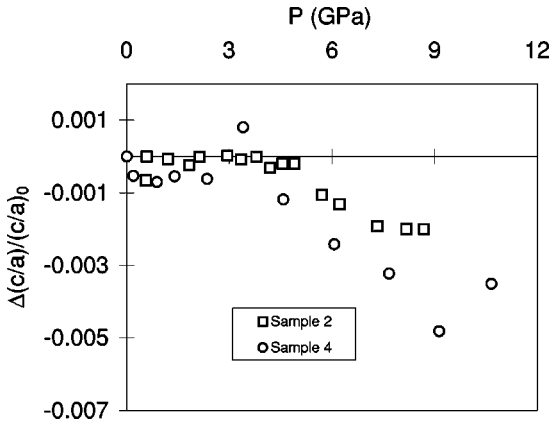

FIG. 6. Variation as a function of pressure of the axial ratio c/a in synthetic wurtzite ZnS.

sure relative volume of 0.821 by fixing $[\partial(B_0)/\partial P]_T=4$ [note: by allowing all three parameters to vary we find $B_0=96.2$ GPa, $V/V_0=0.830$, and $[\partial(B_0)/\partial P]_T=4.35$]. The resulting equation of state is plotted in Fig. 4.

Volume data points of the rocksalt phase follow exactly the same equation of state upon pressure release, as illustrated in Fig. 5. A significant deviation from the extrapolated equation of state, corresponding to the rocksalt phase, is observed, however, for data points in the pressure range where coexist both the rocksalt and the wurtzite phases on pressure release. This point is illustrated in Fig. 5 where the fitted Birch-Murnaghan equations of state of Fig. 4 for both phases are plotted along with the volume-pressure data points recorded upon pressure decrease. The following facts are inferred to understand this observation: (1) Pressures reported are those measured from the pressure gauge, external to the ZnS sample; they represent an average pressure submitted to the ZnS grains and domains; (2) the large volume change between the two structures necessarily lead to a nonaccurate estimation of the pressure encountered by each grains or domains in their respective phase. Hence the measurement of pressure-volume data points in the advent of a multiphase coexistence is always difficult.

Finally, our results for the compression parameters for the wurtzite, zinc-blende, and rocksalt phases are in relatively good agreement with other experimental data (not obtained with synchrotron radiation) and simulated data, as reported in Table III.

C. c/a structural parameter of the wurtzite phase

The measured wurtzite axial ratio is slightly higher ($c/a=1.637$ and $u=(\frac{3}{8})^{1/2}(a/c)=0.374$) than the ideal value ($c/a=1.633$). It is comparable, however, to the axial ratio measured by neutron diffraction, i.e, 1.6377.[22] The relative variation as a function of pressure of the hexagonal structure axial ratio c/a, shown in Fig. 6, indicates a peculiar change. Although the data points are scattered, they indicate a constant relative axial ratio for pressures below 5 GPa followed by a small but definite drop up to 10 GPa. Beyond 11 GPa (data points are not shown in Fig. 6), the wurtzite/rocksalt x-ray-diffraction pattern overlap makes difficult the determination of the structural parameters of either phase; consequently the c/a has not been measured for a pressure range where phase coexistence occurs. A pressure-induced change of the axial ratio as also been reported in wurtzite ZnO. Recent studies in the case of ZnO indicate, however, a linear relationship between the c/a and pressure.[23,24] It should be

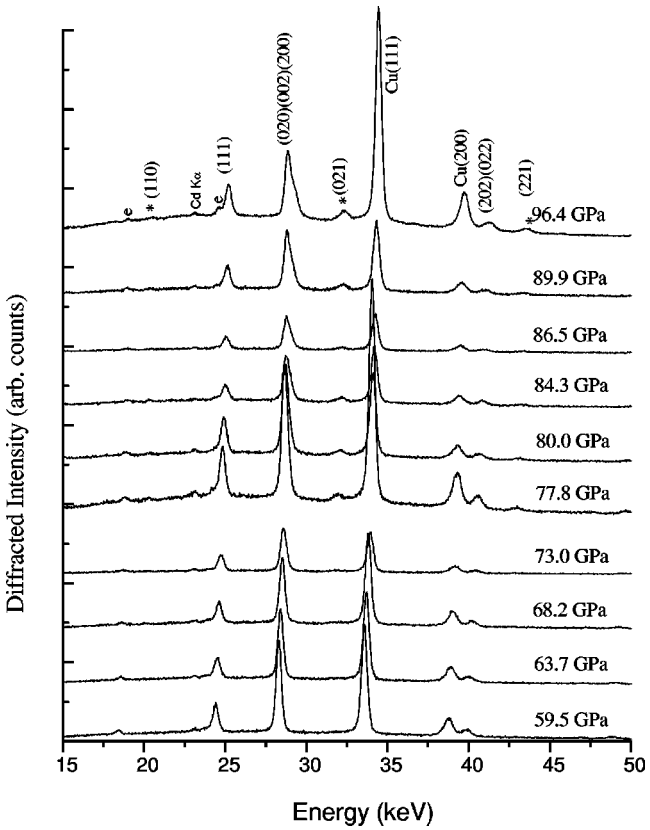

FIG. 7. EDXD spectra of ZnS at selected increases pressures. $Ed=64.861\pm0.005$ keV Å . The sequence indicates the emergence of nonrocksalt diffraction lines (labeled as *), indicative of a transition of rocksalt ZnS to a distorted cubic structure. The transition is entirely reversible.

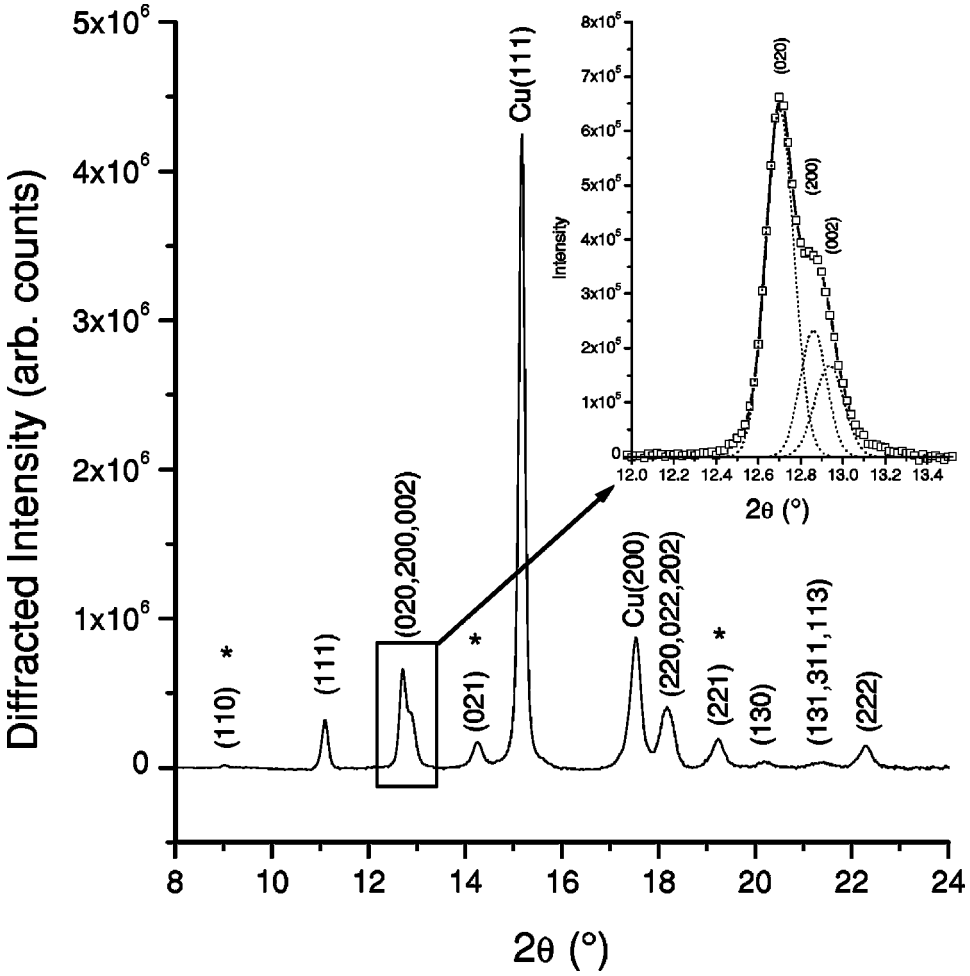

FIG. 8. Angle dispersive x-ray-diffraction pattern of ZnS at 96 GPa (sample 5). The pattern was obtained from an x-ray-diffraction image recorded on an imaging plate at the CHESS B2 station with $\lambda = 0.4659$-Å radiation. X-ray-diffraction lines belonging to the *Cmcm* phase and distinct from the rocksalt structure are indicated by an asterisk. Note also (inset) the splitting of the original rocksalt (200) line as a clear indication of the orthorhombic distortion of the rocksalt structure at that pressure. The lattice parameter refinement gives 4.438(1), 4.486(1), and 4.412(1) Å for *a*, *b*, and *c*, respectively.

noted that the change of the c/a in ZnS occurs within a pressure range where only the low-density wurtzite and zinc blende exist. Consequently, the relative change of c/a measured in ZnS cannot be attributed to a misreading of the pressure due to the coexistence of phases presenting substantially different atomic volumes and is most likely intrinsic.

D. Is there an intermediate phase?

Rigorous searches along the 300-K isotherm as a function of pressure have given no indication of the existence of the cinnabar structure in ZnS, an intermediate phase occurring between the zinc blende and the rocksalt over the 11.4 and 14.5 GPa pressure range, as first suggested by the *ab intitio* pseudopotential calculations of Nazzal and Qteish.[11] An improved calculation by the same authors[12] has indicated that the cinnabar structure does not represent a stable phase of ZnS. The pressure was increased and decreased by steps of ~ 0.5 GPa on most samples and by ~ 0.1 GPa on one sample to ensure that a new phase with a restricted pressure stability range would not be overlooked. It should be mentioned that the cinnabar structure reported in CdTe was observed to cover a small pressure range of tenths of GPa.[25] Furthermore, a cinnabar structure has also been observed in GaAs, intermediate to GaAs-II and GaAs-I upon pressure download.[26] Figure 2 shows representative ADXD patterns from natural ZnS at selected pressures, within the range where the cinnabar phase has been first predicted to be stable. Clearly, starting from the zinc-blende structure, ZnS transforms unambiguously to the rocksalt structure upon pressure increase at room temperature. The back transformation (rocksalt to zinc blende) has been observed upon pressure decrease and proceeds without an intermediate phase.

E. Distortion of the rocksalt structure at higher pressure, above 65 GPa

A transition to a distorted rocksalt structure from the ideal cubic case, starting from 65 GPa, was noted in a preliminary study reported by Nelmes and McMahon.[7] The observation of x-ray diffraction lines additional to those corresponding to the rocksalt, and a slight assymmetric broadening of the (200) line, for instance, at 84 GPa, led the authors to elude to the possibility of a transition to a *Cmcm* structure, an orthorhombic distortion of the rocksalt structure. It is also worth mentioning that Uchino *et al.*[8] have reported the stability of the rocksalt structure of ZnS to 80 GPa (by static compression). Although first assumed to be absent among dense binary systems, the *Cmcm* structure has been observed in numerous III-V and II-VI semiconductors (see Nelmes and McMahon[7] and references therein), and especially in dense CdS, CdSe, CdTe, ZnSe, and ZnTe which bear close resemblance to ZnS as they all transform from their room condition zinc-blende or wurtzite structure to rocksalt structure prior to adopting the *Cmcm* phase at higher density. The observation of the *Cmcm* in ZnS is thus expected.

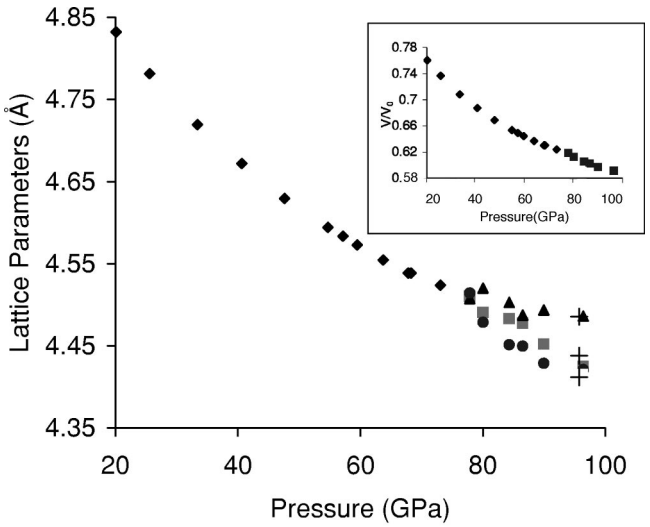

FIG. 9. Variation of the lattice parameters in the rocksalt (a axis: diamonds) and distorted rocksalt ($Cmcm$) phase (a axis: squares; b axis: triangles; and c axis: circles) as a function of increasing pressure obtained by EDXD. The inset shows the calculated relative change of volume (V_0 in given in Table III) along the same pressure range. ADXD data are also plotted (+ symbols). Although the $Cmcm$ phase coexists with the rocksalt phase at a pressure starting from ~ 65 GPa, its structural parameters could be determined only for pressures above 78 GPa. Consequently, only data points corresponding to the rocksalt phase are plotted below 78 GPa. Furthermore, because the orthorhombic distortion remains small with increasing pressure, the accurate determination of the lattice parameters has not been possible and consequently the data points are scattered.

We have recorded clear indications that the rocksalt phase in ZnS is unstable against pressures in excess of 65 GPa. Figure 7 shows selected EDXD spectra which corroborate the rocksalt-to-distorted-rocksalt transition. It is first noted that the additional x-ray diffraction lines are recorded starting from 65 GPa and become more promiment as the pressure reaches the approximate maximum of 96 GPa. The x-ray diffraction lines arise from the shift of alternate Zn and S layers along the b axis: the x-ray-diffraction pattern of the distorted structure resembles that of the rocksalt structure except that, for instance, the (110), (021), and (221) lines are not extinct. The additional x-ray-diffraction lines are in accordance to the conditions $h+k=2n$ in hkl and $h, k=2n$ in $h0l$ and $0kl$, respectively, of space group $Cmcm$ with the two atomic species located on sites $4(c)$ with $(0,y_1,0.25)$ and $(0,y_2,0.25)$.[27] As noted by Nelmes and McMahon,[7] for $a=b=c$ and $y_1=1-y_2=0.75$, the $Cmcm$ structure is then identical to the rocksalt structure. The $Cmcm$ structure is therefore characterized by the shift along the b axis with $y_1=1-y_2\neq 0.75$ and with another possible distortion arising from the fact that y_1-y_2 can be different from 0.5 resulting in a nonlinear chain of atoms along the a axis. The ZnS in the $Cmcm$ structure is illustrated in Fig. 1. A further modification to the cubic rocksalt pattern is observed: the (200) begins to split, clearly observable starting from 75 GPa. At 96 GPa, the highest pressure reached in the present study, the initial cubic (200) line has then become a definite triplet, as inferred by a line profile decomposition with a proper constraint on the x-ray-diffraction linewidth and illustrated in Fig. 8, consequently ruling out the possibility of a transformation to the β-tin structure. The extent of the orthorhombic distortion in dense ZnS above 65 GPa is shown in Fig. 9 where the change of lattice parameters and the relative volume is plotted against pressure. Further data and analysis are needed to estimate the atomic positions. The equation of state of the dense ZnS in the $Cmcm$ structure was not calculated due to the relatively small pressure range over which it was recorded. In brief, like other zinc and cadmium chalcogenides, ZnS transforms to the $Cmcm$ strucutre at high pressure. As a final comment, we note that the stability of the $Cmcm$ phase has never, to our knowledge, been observed from numerical simulations.

IV. SUMMARY

In this study, x-ray diffraction by synchrotron radiation has been used to study the stability and the compressive properties of the dense phases of ZnS at room temperature. ZnS has been shown to transform to the rocksalt structure from its ambient wurtzite or zinc-blende phase at 12.2 ± 0.5 GPa with volume change close to 17%. Using the Birch-Murnaghan equation of state, the following compression parameters evaluated at room conditions have been obtained for the wurtzite, zinc-blende, and rocksalt phases: $B_0=79.5$ GPa, $B_0=80.1$ GPa, and $B_0=117.6$ GPa, respectively, while B_0' is constraint to 4. The rocksalt phase has been found to be stable from 14 to ~ 65 GPa, above which a pressure-enhanced orthorhombic distortion (the $Cmcm$ structure) prevails. Consequently, dense ZnS is similar to the other Zn and Cd chalcogenides with regards to the pressure-induced structure sequence follows: zinc blende/wurtzite $\rightarrow$ rocksalt $\rightarrow Cmcm$. The low-density wurtzite and zinc-blende phases proceed directly to the high-density rocksalt phase upon the application of pressure with no indication of an intermediate cinnabar-type structure phase. At room temperature, the stability of a cinnabar-type structure in ZnS is hence ruled out.

ACKNOWLEDGMENTS

The authors acknowledge the invaluable help of Dr. K. E. Brister, Dr. K. Finkelstein, Dr. C.-S. Zha, and staff members at the Cornell High Energy Synchrotron Source. This work was financially supported by the Natural Sciences and Engineering Research Council of Canada (NSERC).

*Present address: Physics Department, Dalhousie University, Halifax, NS, Canada B3H 3J5.

[1] E. Chang and G. R. Barsch, J. Phys. Chem. Solids **34**, 1543 (1973).

[2] P. L. Smith and J. E. Martin, Phys. Lett. **19**, 541 (1965).

[3] G. J. Piermarini, S. Block, J. D. Barnett, and R. A. Forman, J. Appl. Phys. **46**, 2774 (1975).

[4] S. Block, R. A. Forman, and G. J. Piermarini, in *High Pressure Research Application in Geophysics* (Academic Press, New York, 1977).

[5] S. Ves, U. Schwarz, N. E. Christensen, K. Syassen, and M. Cardona, Phys. Rev. B **42**, 9113 (1990).
[6] Y. Zhou, A. J. Campbell, and D. L. Heinz, J. Phys. Chem. Solids **52**, 821 (1991).
[7] R. J. Nelmes and M. I. McMahon, in *Semiconductors and Semimetals* (Academic Press, New York, 1998), Vol. 54, Chap. 3, pp. 145–246.
[8] M. Uchino, T. Mashimo, M. Kodama, T. Kobayashi, E. Takasawa, T. Sekine, Y. Noguchi, H. Hikosaka, K. Fukuoka, Y. Syono, T. Kondo, and T. Yagi, J. Phys. Chem. Solids **60**, 827 (1999).
[9] J. E. Jaffe, R. Pandey, and M. J. Seel, Phys. Rev. B **47**, 6299 (1993).
[10] J. M. Recio, R. Pandey, and V. Luaña, Phys. Rev. B **47**, 3401 (1993).
[11] A. Nazzal and A. Qteish, Phys. Rev. B **53**, 8262 (1996).
[12] A. Qteish, M. Abu-Jafar, and A. Nazzal, J. Phys.: Condens. Matter **10**, 5069 (1998).
[13] *High-Velocity Impact Phenomena*, edited by R. Kinslow (Academic Press, New York, 1970).
[14] A. C. Mitchell and W. J. Nellis, J. Appl. Phys. **52**, 3363 (1981).
[15] W. J. Nellis, J. A. Moriarty, A. C. Mitchell, M. Ross, R. G. Dandrea, N. W. Ashcroft, N. C. Holmes, and R. G. Gathers, Phys. Rev. Lett. **60**, 1414 (1988).
[16] K. E. Brister, Y. K. Vohra, and A. L. Ruoff, Rev. Sci. Instrum. **57**, 2560 (1986).
[17] S. Desgreniers and K. Lagarec, technical report, LPSD/Université d'Ottawa (unpublished); see also http://www.physics.uottawa.ca/~lpsd/simpa/simpa.htm
[18] S. Desgreniers and K. Lagarec, J. Appl. Crystallogr. **27**, 432 (1994).
[19] S. Desgreniers and K. Lagarec, J. Appl. Crystallogr. **31**, 109 (1998).
[20] R. A. Young, A. Sakthivel, T. S. Moss, and C. Paiva-Santos, technical report, School of Physics, Georgia Institute of Technology (unpublished).
[21] C. H. Bates, W. B. White, and R. Roy, Science **137**, 993 (1962).
[22] E. Kisi and M. M. Elcombe, Acta Crystallogr., Sect. C: Cryst. Struct. Commun. **45**, 1867 (1989).
[23] H. Karzel, W. Potzel, M. Köfferlein, W. Schiessl, M. Steiner, U. Hiller, G. M. Kalvius, D. W. Mitchell, T. P. Das, P. Blaha, K. Schwarz, and M. P. Pasternak, Phys. Rev. B **53**, 11 425 (1996).
[24] S. Desgreniers, Phys. Rev. B **58**, 14 102 (1998).
[25] R. J. Nelmes, M. I. McMahon, N. G. Wright, and D. R. Allan, Phys. Rev. B **48**, 1314 (1993).
[26] M. I. McMahon and R. J. Nelmes, Phys. Rev. Lett. **78**, 3697 (1997).
[27] *International Tables for Crystallography*, 4th ed., edited by T. Hahn (Kluwer Academic Publishers, London, 1995), Vol. A.